



The catalysts supported on metallized electrospun polyacrylonitrile fibrous mats for methanol oxidation

Xiaomin Liu, Miaoyu Li, Gaoyi Han*, Jianhua Dong

Institute of Molecular Science, Key Laboratory of Chemical Biology and Molecular Engineering of Education Ministry, Shanxi University, Wucheng Road, Taiyuan 030006, PR China

ARTICLE INFO

Article history:

Received 8 October 2009
Received in revised form 3 January 2010
Accepted 5 January 2010
Available online 14 January 2010

Keywords:

Electrospinning
Polyacrylonitrile
Methanol electro-oxidation
Gold
Platinum

ABSTRACT

Polyacrylonitrile nanofibrous mats coated with continuous thin gold films (Au-PAN) have been fabricated by combining the electrospinning and electroless plating techniques. The Pt particles are electrodeposited on the Au-PAN fibers surface by multi-cycle CV method, and the Au-PAN decorated with Pt (Pt/Au-PAN) shows higher activity toward methanol electro-oxidation. The catalytic peak current for methanol oxidation on the optimum Pt/Au-PAN electrode can reach about $450 \text{ mA mg}^{-1} \text{ Pt}$ which is much larger than the catalytic peak current for methanol oxidation ($118.4 \text{ mA mg}^{-1} \text{ Pt}$) on the electrode prepared by loading commercial Pt/C on Au-PAN (Pt/C/Au-PAN). Further experiments reveal that the Pt/Au-PAN electrodes exhibit better stability and smaller charge transfer resistance than Pt/C/Au-PAN electrodes, which indicates that the Au-PAN may be developed as supporting material for catalyst. The microscopy images of the electrodes show that the Pt particles deposited on Au-PAN conglomerate into larger particles, and that the Pt/C catalyst loaded on the Au-PAN also exhibits conglomeration after stability test. The hydrogen adsorption–desorption experiments indicate that the electrochemical surface area of the Pt particles for the both kinds of electrodes has decreased after stability test.

© 2010 Elsevier Ltd. All rights reserved.

1. Introduction

Direct methanol fuel cell (DMFC) is considered as one of the most promising options for solving energy crisis in future because of the high-energy conversion efficiency, low-pollutant emission, low operating temperature, simplicity for handling and processing of liquid fuel [1–3]. For the standard DMFC device, platinum-based particles dispersed on carbon materials are usually employed as catalysts for methanol oxidation and oxygen reduction because of their excellent performance in catalysis [4,5]. However, such disadvantages of the catalyst supported on carbon as high cost of noble metal, poor loading and weak dispersion prevent the DMFC from commercializing [6].

It has been recognized that the performance of DMFC would be affected by the support of the catalysts, and that different structures of supports such as carbon black, carbon nanotubes (CNTs), graphite nanofibers, hollow carbon sphere and micro-composite PPy/PS with micro-size will influence not only the structure of the catalyst layer but also the electrochemical performance of the fuel cell [7–12]. Furthermore, recent research reveals that the detachment of catalyst from the supporting materials will make

the catalyst isolated electrically, which can result in a rapid degradation of the Pt catalyst and thus affect its performance [13,14]. So the selection and the preparation of the support for Pt-based catalyst is a key problem to increase the catalytic activity and durability [15,16]. Another key problem for Pt-based catalyst used in DMFC is the strong adsorbing intermediate (CO, HCOOH, etc.) on the catalyst surface, which blocks the active sites from further methanol adsorption and leads to a decrease in the activity [17]. To solve the problems, binary or ternary Pt-based electro-catalysts with an additional metal are considered to be promising and such catalyst as Pt–Ru, Pt–Pd, Pt–Sn, Pt–Au, Pt–Ru–W, Pt–Ru–Mo, etc. have been prepared and evaluated [18–28]. Moreover, bimetallic nanoparticles (NPs) without carbon supports have attracted much attention for being used as electro-catalysts, selective oxidation, and dehydrogenation catalysts [29–32]. But up to the present, there are very few reports about depositing Pt onto Au particles as catalysts [33–35].

On the other hand, electrospun nanofibrous mats have proven to be efficient catalytic supports owing to the high porosity and large surface areas [36,37]. Recently, the conductive fibrous mats have been used as supports for catalytic electrodes [38–40]. However, there are no literatures on using gold-coated PAN nanofibrous mats (Au-PAN) as support for Pt catalytic particles. Considering the high porosity and large surface area of the fibrous mats, close contact between the electrodeposited Pt particles and the fibers, the Pt/Au-PAN catalytic electrodes have been fabricated in this

* Corresponding author. Tel.: +86 137 53497902; fax: +86 351 7016358.
E-mail address: han.gaoyis@sxu.edu.cn (G. Han).

paper through two steps: (1) the continuous thin gold films are electroless-deposited on the PAN electrospun fibers to form the Au-PAN fibrous mats and (2) the Pt particles are electrodeposited on the Au-PAN fibers. As a result, the catalytic electrodes fabricated on the gold-coated fibrous mats will exhibit a high activity for methanol oxidation.

2. Experimental

2.1. Reagents

Polyacrylonitrile (PAN), sodium borohydride and Nafion (5%) solution were obtained from Aldrich. The chemicals of chloroauric acid, oxammonium hydrochloride, chloroplatinic acid and tetrabutyl-ammonium bromide (TBAB) were purchased from Beijing Chemical Company. The commercial Pt/C (40 wt%) was obtained from Johnson Matthey Corp., and all other chemicals employed in this study were of analytical grade.

2.2. Fabrication of the catalytic electrodes

The gold-coated electrospun PAN fibrous mats were prepared by using the method similar to the previous reports [40,41]. The resulted mats were cut into strips with the size of 10 mm × 2.0 mm, then clamped by a clamp and used as working electrode whose geometric surfaces immersed in electrolyte solution were measured to be about 4 mm². The Pt particles were deposited on the mats by using multi-cycle voltammetry method in 0.5 M H₂SO₄ + 2.0 mM H₂PtCl₆ aqueous solutions. The potential window and the scan rate of the potential were optimized as -0.3–0.4 V and 100 mV s⁻¹, respectively. The obtained catalytic electrodes were denoted as Pt/Au-PAN. By comparison, the commercial Pt/C was loaded on the Au-PAN and the electrodes were labeled as Pt/C/Au-PAN, which were fabricated by transferring 10.6 μl of the ultrasonic-treated mixture of Pt/C catalyst (10.0 mg), water (2.5 mL) and Nafion solution (0.5 mL) onto the Au-PAN, and then evaporating the solvent in the air. The content of Pt on the both kinds of electrodes was kept to be about 355.5 μg cm⁻².

2.3. Characterization and electrochemical measurements

Scanning electron microscopy (SEM) and transmission electron microscopy (TEM) micrographs were taken on JEOL-JSM-6700F scanning electron microanalyser and JEM-100CX microscope, respectively. XRD patterns were recorded on Bruker D8 Advance X-ray diffractometer (Cu Ka) with graphite monochromator and films accessory. The contents of platinum were determined by an IRIS Advantage inductively coupled plasma atomic emission spectroscopy (ICP-AES) system. The electro-deposition and electrochemical measurements were carried out on a CHI 660B electrochemistry workstation at 30 °C. The Au-PAN fibrous mats loaded with Pt or Pt/C, a platinum plate and a saturated calomel electrode (SCE) were used as working, counter and reference electrode, respectively. Electrochemical impedance spectroscopy (EIS) was performed with amplitude of 5 mV in the frequency range 100 kHz–0.1 Hz and was carried out at different potentials where a SCE was also used as reference electrode. The Zview-2 fitting program was used to analyze the impedance parameters. The electrolyte for electro-deposition was 0.5 M H₂SO₄ aqueous solution containing 2.0 mM H₂PtCl₆, and for electrodes evaluation was 0.5 M H₂SO₄ + 1.0 M CH₃OH aqueous solution. High-purity argon flow was used for deaerating the solutions and maintained above the electrolyte solution during the measurements.

3. Results and discussion

3.1. The characterization of Au-PAN and Pt/Au-PAN fibrous mats electrode

The obtained nonwoven PAN fibrous mats coated with continuous thin gold films (Au-PAN) with the thickness of about 10 μm and the conductivity of about 1 × 10⁴ S cm⁻¹, show a typical gold-yellow reflective surface. The typical morphology of Au-PAN is shown in Fig. 1A, from which we can find that the random ranked fibers form many gaps on the surface of the mats and that the Au-PAN fibers exhibit a coarse surface whose diameters are fairly uniform and the average diameter is about 740 nm. According to the literature [40], the electrochemical surface areas of the deposited gold in the mats are about 19.8 cm² per 1.0 cm² of geometric surface area. It can be seen from Fig. 1B that the gaps dispersed on the mats become smaller, and that the average diameter of the fibers decorated with platinum in Pt/Au-PAN increases to about 810 nm (90 cycles CV). The diffraction peaks located at about 38.3°, 44.5°, 64.7° and 77.6° in the XRD pattern for Au-PAN are corresponding to the diffraction of Au (1 1 1), (2 0 0), (2 2 0) and (3 1 1) crystal planes, respectively (Fig. 2a). The average diameter of Au particles deposited on the PAN fibers is calculated to be about 22 nm according to the Scherrer formula ($d = 0.89\lambda / B \cos \theta$). The XRD patterns for Pt/Au-PAN (Fig. 2b) and Pt/C/Au-PAN (Fig. 2c) electrodes are similar to that for Au-PAN except that the small diffraction peaks related to Pt (1 1 1) plane are observed at about 39.9° clearly whose intensities are about one tenth of the intensity of Au(1 1 1). The average diameters of the Pt particles are calculated to be about 7.5 nm and 4.2 nm for Pt/Au-PAN and Pt/C/Au-PAN, respectively. The similar XRD pattern for Pt–Au electrode has also been observed previously [17]. We can also find that the Pt particles deposited (90 cycles CV) on the gold films have almost no influence on the average diameter of the gold particles (23 nm).

3.2. Electrocatalytic properties of the fibrous mats electrode and the changes of the electrodes after the stability test for methanol oxidation

Fig. 3A shows the relationship between the numbers of the CV cycle for depositing Pt on Au-PAN and the peak current of the methanol oxidation, from which we find that the optimum response current of methanol oxidation can reach to 159.7 mA cm⁻² based on the geometric surface area for Pt/Au-PAN catalytic electrode prepared by 90 cycles CV. In this case, the Pt electrodeposited on the Au-PAN is determined to be about 0.355 mg cm⁻², so the peak current can also be denoted as 450 mA mg⁻¹ Pt which is slightly larger than that of Pt deposited on carbon fibrous mats [7]. The activity of the electrodes will reach maximum at certain number of CV cycles when the catalyst particles are electrodeposited on the supports by multi-CV process, which has also been observed in other reports [7,17]. Then in the following experiments, the Pt/Au-PAN electrodes prepared by 90 cycles CV are chosen as testing electrodes. In 0.5 M H₂SO₄ + 1.0 M CH₃OH aqueous solutions, the curve for Au-PAN electrode shows no significant redox response (Fig. 3B-a) to methanol oxidation. However, the anodic current density on Pt/Au-PAN electrode in the positively going scan increases with the increase of scan potential, and the peak current density reaches to 159.7 mA cm⁻² (450 mA mg⁻¹ Pt) at 0.73 V (Fig. 3B-c), which is significantly higher than 42.1 mA cm⁻² (118.4 mA mg⁻¹ Pt) at 0.69 V on Pt/C/Au-PAN electrodes (Fig. 3B-b). In the reverse scan there is another anodic peak observed on both Pt/Au-PAN and Pt/C/Au-PAN electrodes, which can be attributed to the removal of the incompletely oxidized carbonaceous species formed in the positively going scan [42]. The electro-oxidation of methanol has been studied extensively and the

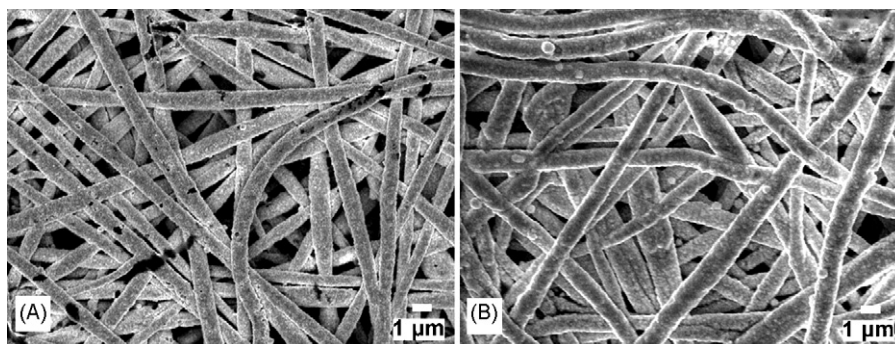


Fig. 1. The SEM images of the Au-PAN fibrous mats as prepared (A) and Pt/Au-PAN prepared by 90 cycles CV (B).

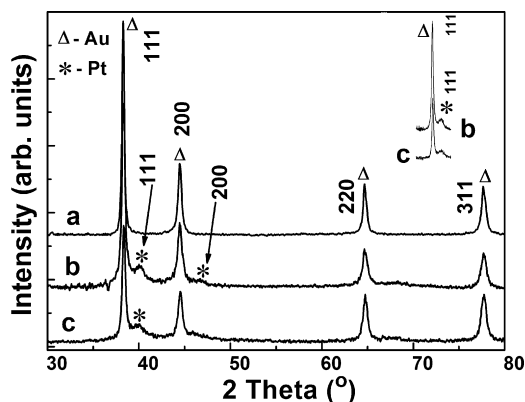
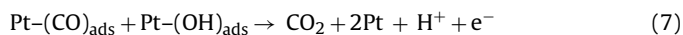
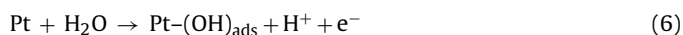
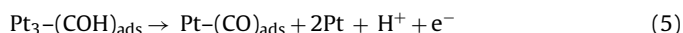
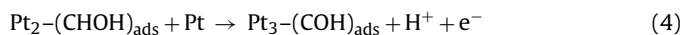


Fig. 2. The XRD patterns of the Au-PAN fibrous mats (a), Pt/Au-PAN prepared by 90 cycles CV (b) and Pt/C/Au-PAN electrode (c).

anodic oxidation of methanol can be written [43,44] as:



In acid media, the reaction has been suggested to follow the series of steps during the process of oxidation:



The anodic peak current densities in the positively and negatively going scan are defined as I_f and I_b , and the value of I_f/I_b

can be used to evaluate the tolerance of catalyst to the accumulation of the carbonaceous species [45,46]. In this case, the value of I_f/I_b (1.08) for the Pt/Au-PAN electrode is obviously larger than that (0.80) for Pt loaded on the carbon material [7,39] and smaller than that (1.9) for Pt–Au porous electrode reported previously [17], suggesting that the Pt/Au-PAN electrodes have slight effect in reducing the absorbed carbon monoxide.

Fig. 4A shows the anodic peak current densities of methanol oxidation on Pt/Au-PAN and Pt/C/Au-PAN electrodes during a total of 850 CV cycles in 0.5 M H_2SO_4 + 1.0 M CH_3OH aqueous medium with a scan rate of 100 mV s^{-1} . For the both electrodes, the anodic peak current density in positively going scan increases at initial cycles until it attains the maximum value and afterwards displays a downward trend with the successive CV scans. For Pt/Au-PAN electrode, the peak current density approaches a maximum of 173.1 mA cm^{-2} at the 77th cycle, and then decreases to 101.1 mA cm^{-2} and 91.6 mA cm^{-2} at the 600th and 850th cycles, with a total decrease of 41.6% and 47.1%, respectively. However, the peak current density reaches its maximum (44.6 mA cm^{-2}) at the 111th cycle for Pt/C/Au-PAN electrodes, and then decreases to 18.4 mA cm^{-2} and 10.78 mA cm^{-2} at the 600th and 850th cycles, with a total decrease of 58.7% and 75.8%, respectively. The peak current density loss may result from the consumption of the CH_3OH in solution during the CV scans and be also due to the poisoning and structure changing of Pt catalysts which usually leads to a decrease of the catalytic activity. Fig. 4B shows the curve of the polarization currents density of methanol oxidation versus time at a constant potential of 0.50 V. After reaching their maximums, the current densities of methanol oxidation on both Pt/Au-PAN and Pt/C/Au-PAN electrodes present continuous decay with the increase of time. After a polarization time of 6000 s, there are 2.31 mA cm^{-2} and 0.56 mA cm^{-2} current densities retained on Pt/Au-PAN and Pt/C/Au-PAN electrodes, respectively. In addition, the decay of the current density on Pt/Au-PAN electrode exhibits a more gently decreasing trend. In comparison with the stability test reported

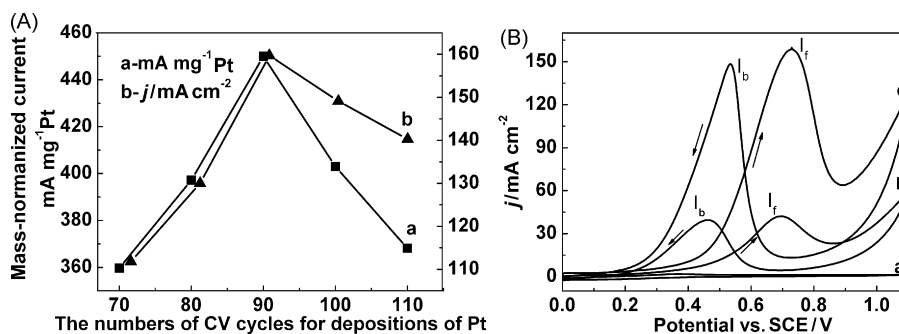


Fig. 3. (A) The plot of the peak current density of methanol oxidation on different Pt/Au-PAN electrodes versus the cycle number of CV for Pt deposition, (B) cyclic voltammograms obtained for methanol oxidation on (a) Au-PAN, (b) Pt/C/Au-PAN and (c) Pt/Au-PAN (Pt deposited by CV with 90 cycles) electrodes with the potential scan rate of 50 mV s^{-1} .

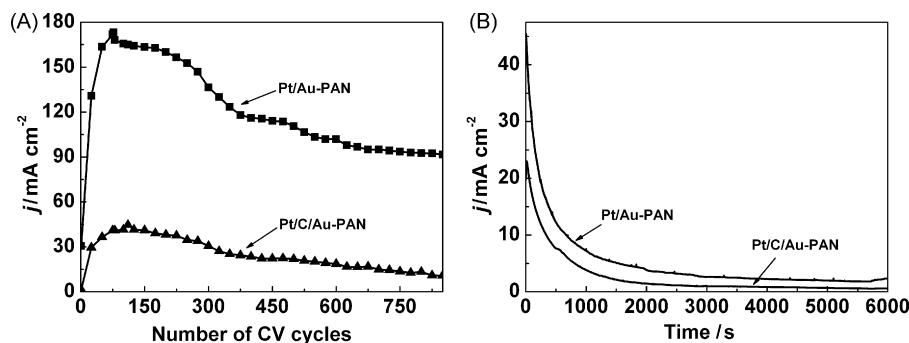


Fig. 4. (A) The plot of anodic peak current density of methanol oxidation on Pt/Au-PAN and Pt/C/Au-PAN electrodes versus cycle numbers with the potential scan rate of 100 mV s^{-1} . (B) Chronoamperometric curves of methanol oxidation on Pt/C/Au-PAN and Pt/Au-PAN at potential of 0.5 V (versus SCE).

previously [7,39], we find that the Pt/Au-PAN electrodes almost has no such synergetic effect as improvement of the stability for Pt particles although the stability of Pt catalyst has been increased by modifying Au on the Pt particles [27,28].

In order to investigate the changes of microstructure on the electrodes, the SEM images of the Pt/Au-PAN and Pt/C/Au-PAN electrodes are recorded after the stability test. We can find from Fig. 5A that the average diameter of the fibers in Pt/Au-PAN electrode is about 808 nm which decreases slightly in comparison with the electrodes as prepared (810 nm), and that many clusters with diameter of 380 nm are observed on the mats surface after the electrode goes through 50 cycles CV. It is amazing that the average diameter of the fibers in Pt/Au-PAN electrode decreases to about 760 nm and the surface of the fibers becomes smooth after stability test (500 cycles CV), and at the same time a lot of larger clusters with size of 350 nm can be observed on the surface of the fibers (Fig. 5B). We can also find that the Pt/C particles are dispersed on the Au-PAN surface smoothly and uniformly for Pt/C/Au-PAN electrode initially (Fig. 5C). However, the Pt/C particles have congregated into larger cluster in some part of the catalyst layer after the stability test, and some cracks are also observed in the catalyst layer (Fig. 5D).

The similar changes can also be observed from the TEM images shown in Fig. 6. For example, we can find that the gold particles form the compact films (Fig. 6A) on the Au-PAN fibers. After Pt particles are deposited by 90 cycles CV, we find that many small particles with a diameter of about $4\text{--}9 \text{ nm}$ (7.5 nm obtained from XRD pattern) disperse on the gold particles surface (Fig. 6B). However, the surface of Pt/Au-PAN fibers becomes smooth (Fig. 6C) after the electrode endures long time CV scan (500 cycles) in comparison with Pt/Au-PAN as prepared. For Pt/C/Au-PAN electrodes, we can find clearly that the larger clusters formed by Pt/C particles cling to the Au-PAN fibers, and that the Pt particles with a diameter of about $2\text{--}6 \text{ nm}$ (the average size is 4.2 nm based on the XRD data) dispersed on the carbon particles can be seen clearly (Fig. 6D). It is surprising that the Pt/C particles attached to the Au-PAN fibers have congregated into compact clusters after the stability test, which causes the Pt particles dispersed on the carbon particles undistinguishably (Fig. 6E).

It is considered that the electrocatalytic activity of the electrodes depends on the electrochemical active surface area (ECSA) of the catalyst, so the hydrogen adsorption–desorption on the electrodes has been measured in deaerated $0.5 \text{ M H}_2\text{SO}_4$ aqueous solution by using cyclic voltammograms method at sweep rate

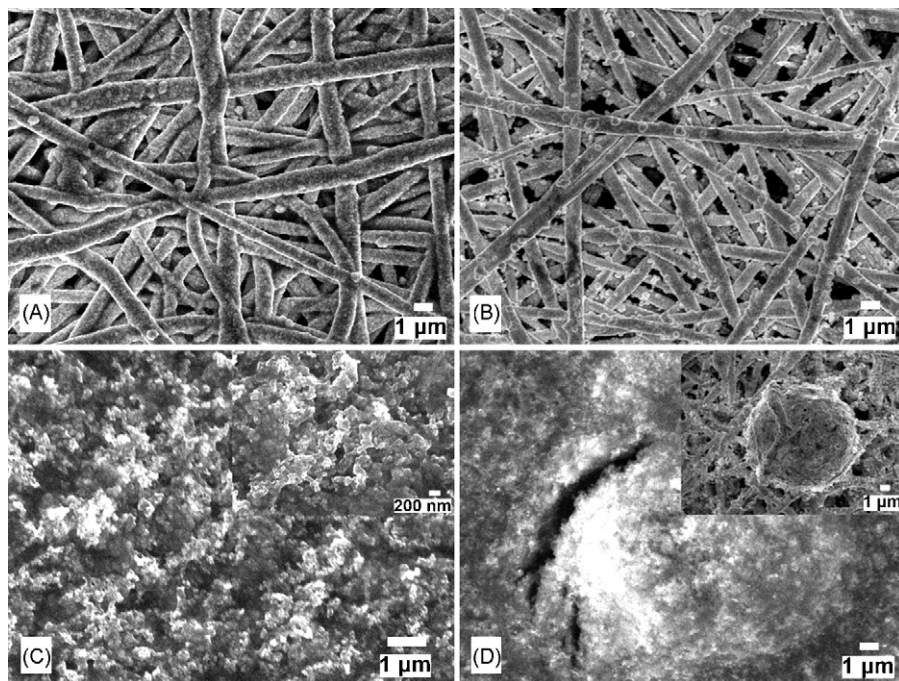


Fig. 5. The SEM images for the Pt/Au-PAN electrode after 50 cycles CV (A) and after the stability test of 500 cycles CV (B), the Pt/C/Au-PAN electrode as prepared (C) and after the stability test of 500 cycles CV (D). The electrolyte is $0.5 \text{ M H}_2\text{SO}_4 + 1.0 \text{ M CH}_3\text{OH}$ and the potential scan rate is 100 mV s^{-1} .

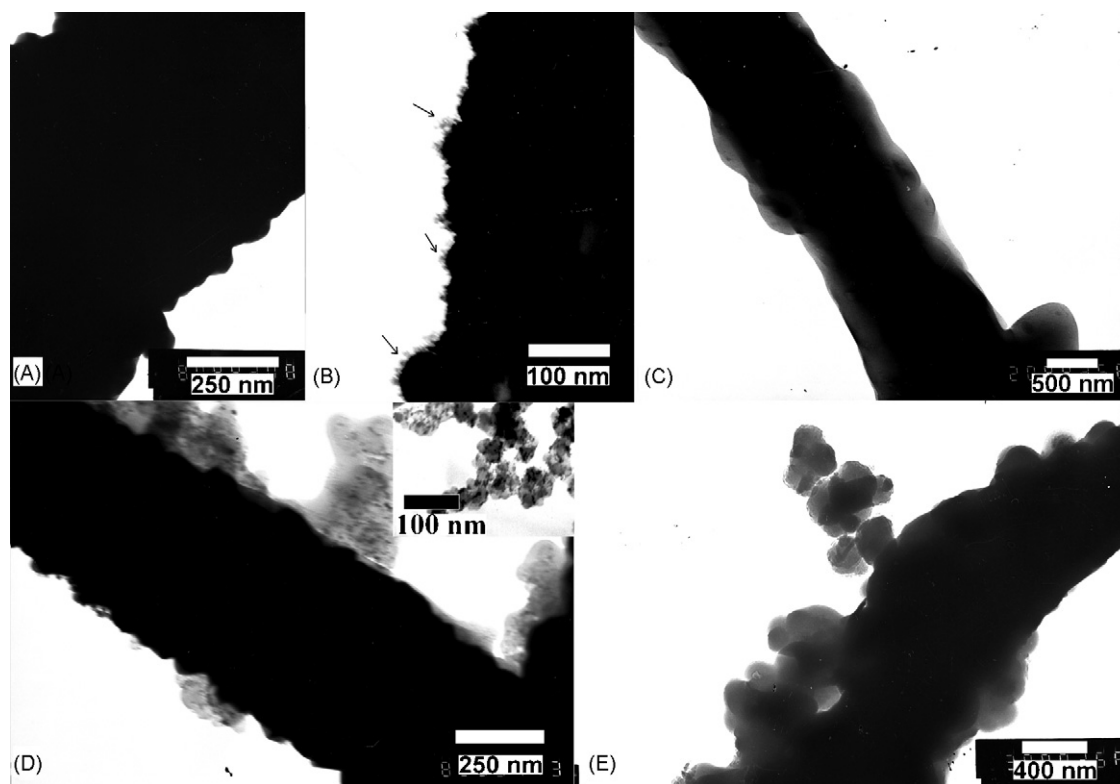


Fig. 6. The TEM images of the Au-PAN fiber as prepared (A), Pt/Au-PAN electrode as prepared (the arrow indicate the platinum particles) (B), the Pt/Au-PAN electrode after stability test (500 cycles CV) (C), the Pt/C/Au-PAN electrode as prepared (inserted figure is the Pt/C TEM image) (D) and the Pt/C/Au-PAN electrode after the stability test (500 cycles CV) (E). The electrolyte is 0.5 M H_2SO_4 + 1.0 M CH_3OH , and the potential scan rate is 100 mV s^{-1} .

of 50 mV s^{-1} . We find from Fig. 7 all electrodes exhibit the features of the hydrogen adsorption–desorption within the region of -0.24 – 0.1 V (versus SCE). Using the data of $210 \mu\text{C cm}^{-2}$ for a clean planar platinum electrode [47], the ECSA of the electrodes is calculated by integrating the area under the hydrogen desorption (-0.24 – 0.1 V). The ECSA for Pt particles electrodeposited on Au-PAN and Pt/C loaded on Au-PAN is calculated as $39.8 \text{ m}^2 \text{ g}^{-1}$ and $30.6 \text{ m}^2 \text{ g}^{-1}$, then decreases to about $30.8 \text{ m}^2 \text{ g}^{-1}$ and $15.4 \text{ m}^2 \text{ g}^{-1}$ after stability test of 50 cycles CV, respectively. The areas of the hydrogen desorption at -0.24 – 0.1 V decrease dramatically and a weak dehydrogenation peak at 0.19 V is observed clearly in the CV curves after 500 cycles CV testing for both Pt/Au-PAN and Pt/C/Au-PAN electrodes. According to the literature [48,49], the hydrogen desorption wave at -0.24 – 0.1 V is corresponding to the Pt nanoparticles as prepared, and the peak at 0.19 V correlates with the hydrogen desorption wave on Pt (111) crystal plane. Furthermore, recent research reveals that the orders of activities

of the Pt catalytic electrodes are Pt nanoparticle \gg Pt (111) \approx Pt (100) $>$ Pt(poly) in methanol oxidation [49]. The results obtained in this paper may indicate that the platinum nanocrystal has been reconstructed during the stability test and the basal plane of Pt (111) becomes the main plane.

It is generally considered that the small Pt particles exhibit higher activity to methanol electro-oxidation than large particles, but the results obtained in this paper are different. In order to explain the reason, such factors as following must be considered: (1) it is unavoidable that a significant portion of Pt/C particles is detached from the substrate and isolated from the electrical circuit even with the most advanced electrodes prepared by wetting–drying method, resulting in a low Pt utilization [13,14], (2) the necessary addition of Nafion for proton transport tends to isolate carbon particles in the catalyst layer, leading to poor electron transport [13], (3) the ECSA measured by the hydrogen adsorption–desorption and the catalytic activity toward

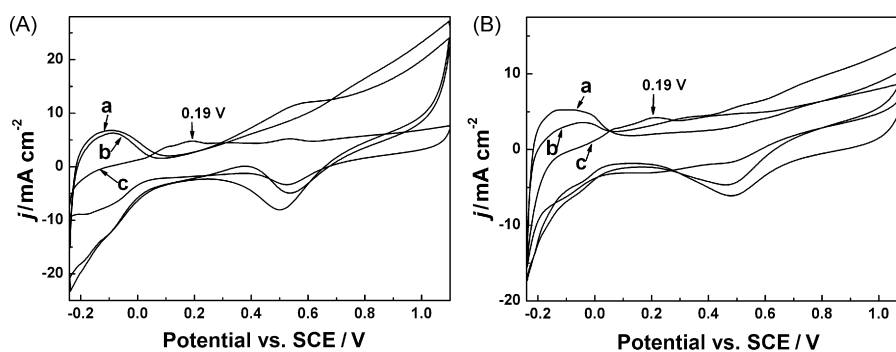


Fig. 7. The cyclic voltammograms for (A) Pt/Au-PAN and (B) Pt/C/Au-PAN catalytic electrodes in Ar-saturated 0.5 M H_2SO_4 solutions with scan rate of 50 mV s^{-1} . The curves (a) the electrodes as prepared, (b) after 50 cycles CV and (c) after 500 cycles CV in 0.5 M H_2SO_4 + 1.0 M CH_3OH with the potential scan rate of 100 mV s^{-1} .

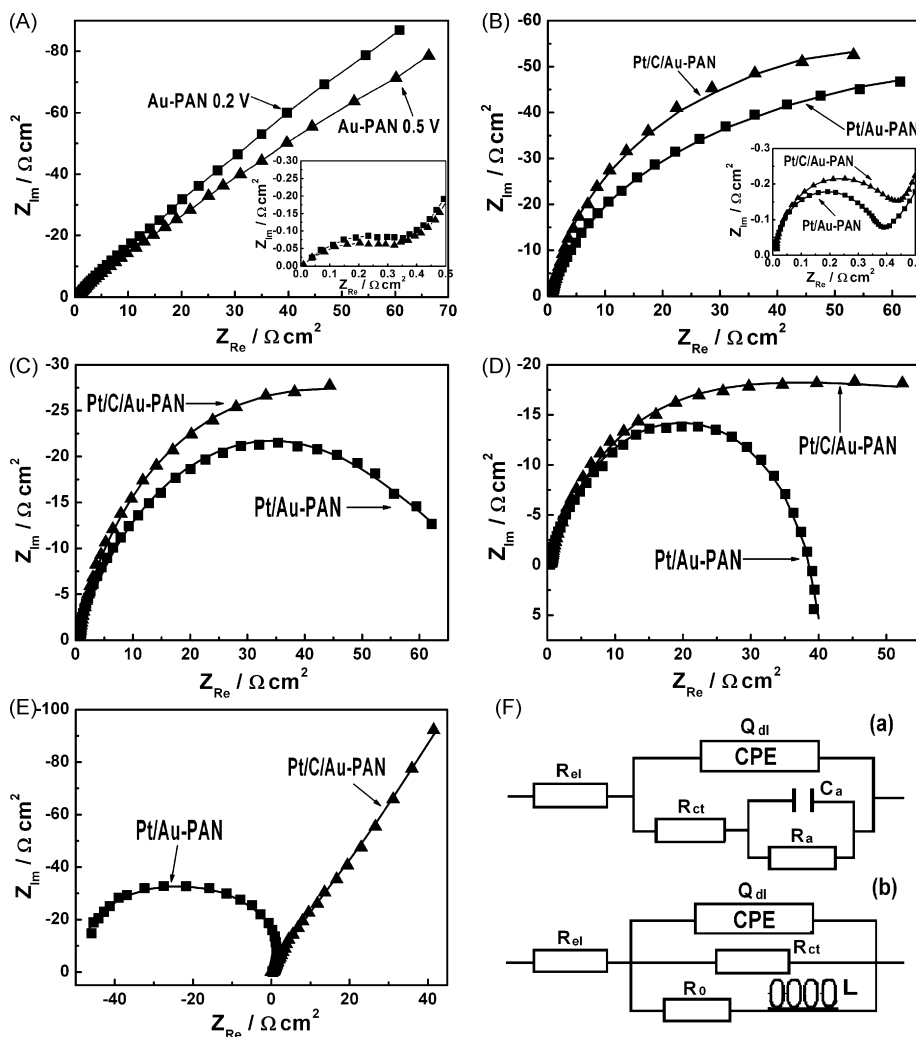


Fig. 8. Complex plane plots of the impedance of the Au-PAN, Pt/Au-PAN and Pt/C/Au-PAN electrodes in 0.5 M H_2SO_4 + 1.0 M CH_3OH aqueous solution. (A) The Au-PAN electrode; the Pt/Au-PAN and Pt/C/Au-PAN electrodes at (B) 0.2 V, (C) 0.4 V, (D) 0.5 V and (E) 0.66 V versus SCE, respectively, (F) the equivalent electrocircuit (a) for (B) and (E), and (b) for (C) and (D), the data signed as (\blacktriangle) and (\blacksquare) are the data obtained from EIS experiments, the lines show the fitted results for B–E. The inserted figures in A and B represent the small semicircle in high frequency region.

methanol oxidation depend on the Pt catalyst particles in the circuit. The conductivity of Pt/Au-PAN is measured to be about 2800 S/cm and smaller than that of Au-PAN, but larger than that of Pt/C/Au-PAN electrodes (1120 S/cm), indicating that the contact resistance between catalyst and substrate in Pt/C/Au-PAN electrodes is larger than in Pt/Au-PAN electrodes assuredly. So the Pt/C particles loaded on the substrate by wetting–drying process exhibit a small ECSA and low catalytic activity to methanol oxidation because the unavoidable detachment of the Pt/C from the substrate and the addition of Nafion for proton transport will lead to a larger contact resistance between the catalyst and support. However, the Pt particles contact with substrate well in Pt/Au-PAN electrodes and the Pt particles can contribute to ECSA and catalysis furthest, so the ECSA and the catalytic activity measured are larger. The similar result has also been observed previously [39], the same commercial Pt/C loaded on the carbon fibrous mats exhibits higher activity than that on carbon paper because the special porous structure of carbon fibrous mats can make the Pt/C catalyst contact the substrate well.

After the stability test, a lot of large particles are observed on the fibers in Pt/Au-PAN electrode, the cracks and larger compact congeries of Pt/C are found in Pt/C/Au-PAN electrode. As a result, the agglomeration and sintering of Pt particles are unavoidable

with the CV scan proceeding in spite of the dispersive form of Pt particles, which may decrease the ECSA and the activity of the catalyst usually [14]. But on the Pt/C/Au-PAN electrodes, besides the unavoidable agglomeration and sintering of Pt particles, the cracks and larger compact congeries of Pt/C are also observed after the stability test (see the SEM and TEM images), which will make the catalyst more isolated electrically. These two factors will result in a rapid degradation of the Pt/C catalyst and thus affect the performance in comparison with the Pt/Au-PAN electrodes.

3.3. Electrochemical impedance spectra

In order to obtain more information about the catalytic electrodes, electrochemical impedance spectra (EIS) are recorded at the same condition. The measurements of EIS, in which the ac impedance is recorded as a function of the ac sources frequency, and from which the charge transfer resistance (R_{ct}) will be obtained [50], can reveal the charge transfer property of methanol oxidation over the Pt/Au-PAN and Pt/C electrodes. From the complex plots of the impedance shown in Fig. 8, we find the Au-PAN electrodes show a small semicircle at high frequency and an arc at low frequency, the complex plots almost have no change with the increase of the potential, indicating that the Au-PAN electrodes almost have no

catalysis for methanol oxidation at present condition (Fig. 8A). We also find that all the complex plots of the impedance for Pt loaded electrodes consist of two semicircles or arcs in which some at the high frequency are independent of potentials and may be associated with a double charging effect, while the other ones (Fig. 8B–E) at low frequency appear to vary with potentials and may associate with the R_{ct} . For example, at potential of 0.2 V, we can find that the Pt/Au-PAN electrodes show the feature corresponding to the capacitive behaviors (Fig. 8B), which signifies a reaction with one adsorbed intermediate. So the methanol dehydrogenation is assumed as rate-determining step during the methanol oxidation process [50,51]. In comparison with Fig. 8B, we find that the diameters of the arcs decrease obviously at potential 0.40 V, indicating that the oxidation of methanol on the electrodes has occurred. It is interesting to find that the impedance data plotted in the complex plane extend into the fourth quadrant for Pt/Au-PAN electrode at potential of 0.5 V, which indicates that the oxidation and removal of CO_{ads} become rate-determining step [51]. When the potential reaches to 0.66 V furthermore, the main semicircle at low frequency in the Nyquist plot flips over to the second quadrant (Fig. 8E) for Pt/Au-PAN electrode. This means that resistance R_{ct} becomes negative, which results from passivation of electrode surface [51–53]. The similar trend of changes has also been observed for Pt/C/Au-PAN electrodes although the changes are not distinct and the diameter of the arcs is larger than that for Pt/Au-PAN electrode. For example, we can find that the diameter of the impedance curve at low frequency only decreases with the increase of the potential at 0.2–0.5 V, but the impedance data plotted in the complex plane do not extend into the fourth quadrant at 0.5 V. Furthermore, the impedance curve at low frequency has only one trend of flipping over to the second quadrant at 0.66 V (Fig. 8E). The R_{ct} value for Pt/Au-PAN electrodes is evaluated as $38 \Omega cm^2$ according to Fig. 8D, which is much smaller than $49 \Omega cm^2$ for Pt/C/Au-PAN electrodes. The impedance data shown in Fig. 8B, E and C, D can be fitted through the equivalent circuit shown in Fig. 8F-a and -b [51], respectively. Therefore it is proved that much faster charge transfer rates occur in the total circuit during methanol electro-oxidation on Pt/Au-PAN electrode. The main reason may be that Pt electrodeposited on Au-PAN fibers contacts with the substrate closely and the Pt particles can contribute to the catalysis furthest, which makes the electron transfer between the catalyst and supporting electrodes easier and causes a smaller R_{ct} value. However, the unavoidable detachment [13,14] of Pt/C from the supporting electrode will increase the total resistance between catalyst and substrate, which causes the electron to transfer from catalyst to supporting electrodes difficultly and cause a larger R_{ct} .

The performance of optimum Pt/Au-PAN electrodes is superior to that of commercial Pt/C loaded on Au-PAN electrode in both the activity and the stability although the platinum particles electrodeposited on the Au-PAN fibers are larger than that of Pt/C. We may conclude that the high performance of the Pt/Au-PAN electrode comes mainly from the close contact between the Pt particles and the Au-PAN fibers, which can make the most catalyst particles contribute to the catalysis furthest. However, a significant part of catalyst is isolated from the circuit and cannot contribute to the catalysis, which causes a low performance on Pt/C/Au-PAN electrodes. The amalgamation of Pt particles in Pt/Au-PAN, the sintering of Pt and the congregation of Pt/C in Pt/C/Au-PAN electrodes cause a rapid degradation of the Pt catalyst.

4. Conclusions

The Au-PAN has been fabricated based on the electrospinning and electroless plating method. The catalytic electrode of Pt/Au-PAN has been fabricated by using the Au-PAN as substrate

through electrochemical deposition. The studies show that the Pt/Au-PAN exhibits high performance in the aspects of electro-catalytic activity and stability toward the oxidation of methanol. The metallized fibrous mats could be developed as a new kind of supporting materials with higher performance for noble metal catalyst.

Acknowledgments

This work is financially supported by the National Natural Science Foundation of China (No. 20604014) and Shanxi province (No. 2007021008), and the Program for the Top Young and Middle-aged Innovative Talents of Higher Learning Institutions of Shanxi (TYMIT and TYAL).

Appendix A. Supplementary data

Supplementary data associated with this article can be found, in the online version, at doi:10.1016/j.electacta.2010.01.014.

References

- [1] Y. Zhao, L.Z. Fan, H.Z. Zhong, Y.F. Li, S.H. Yang, *Adv. Funct. Mater.* 17 (2007) 1537.
- [2] J.K. Lee, J. Choi, S.J. Kang, J.M. Lee, Y. Tak, J. Lee, *Electrochim. Acta* 52 (2007) 2272.
- [3] M. Winter, R.J. Brodd, *Chem. Rev.* 104 (2004) 4245.
- [4] W.Z. Li, C.H. Liang, W.J. Zhou, J.S. Qiu, Z.H. Zhou, G.Q. Sun, Q. Xin, *J. Phys. Chem. B* 107 (2003) 6292.
- [5] S.H. Joo, C. Pak, D.J. You, S.A. Lee, H.I. Lee, J.M. Kim, H. Chang, D. Seung, *Electrochim. Acta* 52 (2006) 1618.
- [6] Z.D. Wei, L.L. Li, Y.H. Luo, C. Yan, C.X. Sun, G.Z. Yin, P.K. Shen, *J. Phys. Chem. B* 110 (2006) 26055.
- [7] M.Y. Li, G.Y. Han, B.S. Yang, *Electrochem. Commun.* 10 (2008) 880.
- [8] Y.H. Lin, X.L. Cui, C. Yen, C.M. Wai, *J. Phys. Chem. B* 109 (2005) 14410.
- [9] F.Y. Xie, H. Meng, P.K. Shen, *Electrochim. Acta* 53 (2008) 5039.
- [10] J. Wu, F.P. Hu, X.D. Hu, Z.D. Wei, P.K. Shen, *Electrochim. Acta* 53 (2008) 8341.
- [11] E. Formo, Z.M. Peng, E. Lee, X.M. Lu, H. Yang, Y.N. Xia, *J. Phys. Chem. C* 112 (2008) 9970.
- [12] H.X. Huang, S.X. Chen, C.E. Yuan, *J. Power Sources* 175 (2008) 166.
- [13] C. Wang, M. Waje, X. Wang, J.M. Tang, R.C. Haddon, Y.S. Yan, *Nano Lett.* 4 (2004) 345.
- [14] S.Y. Huang, P. Ganesan, S. Park, B.N. Popov, *J. Am. Chem. Soc.* 131 (2009) 13898.
- [15] L. Li, Y.C. Xing, *J. Phys. Chem. C* 111 (2007) 2803.
- [16] M.C. Tsai, T.K. Yeh, C.H. Tsai, *Electrochem. Commun.* 8 (2006) 1445.
- [17] J.B. Jia, L.Y. Cao, Z.H. Wang, *Langmuir* 24 (2008) 5932.
- [18] L.H. Jiang, G.Q. Sun, Z.H. Zhou, S.G. Sun, Q. Wang, S.Y. Yan, H.Q. Li, J. Tian, J.S. Guo, B. Zhou, Q. Xin, *J. Phys. Chem. B* 109 (2005) 8774.
- [19] Z.F. Liu, J.E. Hu, Q. Wang, K. Gaskell, A.I. Frenkel, G.S. Jackson, B. Eichhorn, *J. Am. Chem. Soc.* 131 (2009) 6924.
- [20] J.H. Jiang, A. Kucernak, *Electrochem. Commun.* 11 (2009) 623.
- [21] H. Wang, C.W. Xu, F.L. Cheng, M. Zhang, S.Y. Wang, S.P. Jiang, *Electrochem. Commun.* 10 (2008) 1575.
- [22] M.V. Martinez-Huerta, J.L. Rodriguez, N. Tsiouvaras, M.A. Pena, J.L.G. Fierro, E. Pastor, *Chem. Mater.* 20 (2008) 4249.
- [23] E.V. Spinace, L.A. Farias, M. Linardi, A.O. Neto, *Mater. Lett.* 62 (2008) 2103.
- [24] S.H. Liu, W.Y. Yu, C.H. Chen, A.Y. Lo, B.J. Hwang, S.H. Chien, S.B. Liu, *Chem. Mater.* 20 (2008) 1622.
- [25] R. Chetty, K. Scott, *J. Appl. Electrochem.* 37 (2007) 1077.
- [26] D. Zhao, B.Q. Xu, *Angew. Chem. Int. Ed.* 45 (2006) 4955.
- [27] J.B. Xu, T.S. Zhao, Z.X. Liang, L.D. Zhu, *Chem. Mater.* 20 (2008) 1688.
- [28] Z.X. Liang, T.S. Zhao, J.B. Xu, *J. Power Sources* 185 (2008) 166.
- [29] Y.Q. Wang, Z.D. Wei, L. Li, M.B. Ji, Y. Xu, P.K. Shen, J. Zhang, H. Zhang, *J. Phys. Chem. C* 112 (2008) 18672.
- [30] I.S. Park, K.S. Lee, Y.H. Cho, H.Y. Park, Y.E. Sung, *Catal. Today* 132 (2008) 127.
- [31] B.C. Du, Y.Y. Tong, *J. Phys. Chem. B* 109 (2005) 17775.
- [32] D.G. Xia, G. Chen, Z.Y. Wang, J.J. Zhang, S.Q. Hui, D. Ghosh, H.J. Wang, *Chem. Mater.* 18 (2006) 5746.
- [33] J.K. Lee, J. Lee, J. Han, T.H. Lim, Y.E. Sung, Y. Tak, *Electrochim. Acta* 53 (2008) 3474.
- [34] J. Luo, M.M. Maye, V. Petkov, N.N. Kariuki, L.Y. Wang, P. Njoki, D. Mott, Y. Lin, C.J. Zhong, *Chem. Mater.* 17 (2005) 3086.
- [35] J.H. Zeng, J. Yang, J.Y. Lee, W.J. Zhou, *J. Phys. Chem. B* 110 (2006) 24606.
- [36] A. Greiner, J.H. Wendorff, *Angew. Chem. Int. Ed.* 46 (2007) 5670.
- [37] D. Li, Y.N. Xia, *Adv. Mater.* 16 (2004) 1751.
- [38] C. Kim, K.S. Yang, M. Kojima, K. Yoshida, Y.J. Kim, Y.A. Kim, M. Endo, *Adv. Funct. Mater.* 16 (2006) 2393.
- [39] M.Y. Li, S.Z. Zhao, G.Y. Han, B.S. Yang, *J. Power Sources* 191 (2009) 351.
- [40] B. Guo, S.Z. Zhao, G.Y. Han, L.W. Zhang, *Electrochim. Acta* 53 (2008) 5174.

- [41] G.Y. Han, B. Guo, L.W. Zhang, B.S. Yang, *Adv. Mater.* 19 (2006) 1709.
- [42] M.W. Xu, G.Y. Gao, W.J. Zhou, K.F. Zhang, H.L. Li, *J. Power Sources* 175 (2008) 217.
- [43] J.B. Goodenough, A. Hamnett, B.J. Kennedy, S.A. Weeks, *Electrochim. Acta* 32 (1987) 1233.
- [44] B.J. Kennedy, A. Hamnett, *J. Electroanal. Chem.* 283 (1990) 271.
- [45] G.Y. Zhao, C.L. Xu, D.J. Guo, H. Li, H.L. Li, *J. Power Sources* 162 (2006) 492.
- [46] L.J. Zhang, D.G. Xia, *Appl. Surf. Sci.* 252 (2006) 2191.
- [47] D. Villers, S.H. Sun, A.M. Serventi, J.P. Dodelet, *J. Phys. Chem. B* 110 (2006) 259165.
- [48] N. Tian, Z.Y. Zhou, S.G. Sun, *J. Phys. Chem. C* 112 (2008) 19801.
- [49] C.K. Rhee, B.J. Kim, C. Ham, Y.J. Kim, K. Song, K. Kwon, *Langmuir* 25 (2009) 7140.
- [50] E.H. Yu, K. Scott, R.W. Reeve, *J. Electroanal. Chem.* 547 (2003) 17.
- [51] G. Wu, L. Li, B.Q. Xu, *Electrochim. Acta* 50 (2004) 1.
- [52] V.S. Bagotzky, Y.B. Vassilyev, *Electrochim. Acta* 12 (1967) 1323.
- [53] R.E. Melnick, G.T.R. Palmore, *J. Phys. Chem. B* 105 (2001) 9449.